

Valence-bond treatment of distortions in polyacene polymers

M. A. Garcia-Bach and A. Peñaranda

Física Fonamental, Facultat de Física, Universitat de Barcelona, Diagonal 647, 08028 Barcelona, Catalunya, Spain

D. J. Klein

Texas A&M University at Galveston, Galveston, Texas 77553-1675

(Received 8 November 1991; revised manuscript received 28 January 1992)

Distortions of polyacene polymers are studied within a many-body valence-bond framework using a powerful transfer-matrix technique for the valence-bond (or Heisenberg) model of the system. The computations suggest that the ground-state geometry is either totally symmetric or possibly exhibits a slight (A_2 or B_2 symmetry) bond-alternation distortion. The lowest-energy (nonsymmetric, in-plane) distortions are the A_2 and B_2 modes, which, within our approximations, are degenerate.

I. INTRODUCTION

The conductivity of polyacetylene and even superconductivity of several quasi-one-dimensional systems has stimulated extensive investigations on the electrical properties of one-dimensional (1D) systems. Theory for π -electron networks has most commonly been approached via the Hückel crystalline-orbital (CO) model, which, for polymeric systems with translational symmetry, is also termed the simple tight-binding band-theoretic model with interactions limited to nearest neighbors. In such 1D systems this theory has been much developed with the recognition that novel Peierls distortions should often occur. Further, if there are such degenerate distortions, the possibility of solitonic excitations arises.

Since polyacene (Fig. 1) is one of the simpler polymers after polyacetylene, the possibility of Peierls distortions for this system has already been considered several times in terms of the simple Hückel CO model or slight extensions thereof. Indeed, within this model the undistorted species with equal numbers of π electrons and π centers exhibits a zero band gap, as noted by Coulson,¹ McWeeny,² and Moffitt.³ Thence, Salem and Longuet-Higgins⁴ and Kimura *et al.*⁵ found the species to be stable against one distortion involving bond alternation in both the top and the bottom boundary chains of the polymer, while Boon⁶ and others⁷⁻¹⁰ found it to distort (presumably quadratically) in another mode. However, Kivelson and Chapman,¹¹ and Božović,¹² argue for a true Peierls distortion of a different symmetry. Still others¹³⁻¹⁶ investigated the effects of correlation (from a CO view), finding that it introduces a band gap even in the symmetric case, thereby precluding a true Peierls distortion.

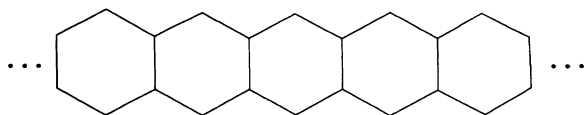


FIG. 1. Five cells of the polyacene chain.

Our purpose is to study polyacene from the limit of strong correlation. In this case, the model space reduces to one electron occupancy per site and applicable effective Hamiltonians are of the Heisenberg type, such as in general derived, e.g., in Refs. 17 or 18, and for the present type of conjugated hydrocarbon case derived, e.g., in Refs. 19–22.

In fact, isotropic Heisenberg models had already been applied successfully in chemistry to π electrons of carbon atoms in conjugated networks under the name of the (Pauling-Wheland) valence-bond (VB) model (see, e.g., Refs. 23–25). There are a range of molecular structures for which many-body treatments have been made only relatively infrequently, though there has been a revival of interest recently, as indicated in Ref. 26. Nevertheless, only qualitative VB consideration seems to have been previously paid^{1,27,28} to the polyacene polymer.

Now the question arises as to which if any of the novel features found for the Hückel model, and related self-consistent-field (SCF) treatments, might also occur for the VB (or Heisenberg) model for polymer systems. Evidently the theoretical tools available to address the questions devolve to what occurs within various approximations. Indeed, within the simplest approximation (of counting Kekulé structures) there appear²⁹ to be qualitative correspondences to what is predicted from the simple Hückel CO model, and in a more quantitative manner correspondences have been found³⁰ for the polyacetylenic VB model. Here it is natural to address the question of Peierls distortions for the polyacene polymer of Fig. 1.

For such VB (isotropic spin- $\frac{1}{2}$) Heisenberg models with antiferromagnetically-signed exchange-coupling parameters, the ground-state solution is generally a nontrivial problem. Configuration-interaction techniques have been pushed³¹ so that systems of about twice the size of those treated two decades ago are solvable for the ground state and a few lower-lying states. This limits systems to about 26 sites with computer effort increasing exponentially fast with system size. Further, these solutions are somewhat decoupled from conceptual insight.

Hence many-body studies, especially for the Heisenberg models of larger π -network systems, are of

relevance. Exact Bethe-*Ansatz* results,³² though long studied, seem to be limited to linear chains. Even the interesting problem of bond alternation in the linear chain has not been treated via this approach. Thus more generally applicable approximate approaches are of relevance.

There are several types of many-body cluster-expanded wave-function *Ansätze* based upon a Néel-state zeroth-order picture. Kasteleyn³³ and Huse and Elser³⁴ have developed one such Néel-state-based *Ansatz*. Others^{35–38} have independently made a modified *Ansatz* wherein pair correlations above a perfect Néel state are limited to nearest neighbors. This *Ansatz* surpasses that of Kasteleyn in accuracy for the linear chain, and in has been extended³⁹ by embedding in a systematic cluster-expansion hierarchy.

With the advent of high-temperature superconductors, Anderson⁴⁰ suggested the relevance of resonating-VB descriptions, and intense worldwide activity on the idea has ensued. Hundreds of papers have appeared, though often they are either of a general nature, sometimes overlapping with much of the earlier work already cited, or are tightly focused on mixed-valence perovskite structures rather than benzenoid ones.

Since polyacene is a bipartite system (with equal numbers of sites in the two parts), it has⁴¹ a singlet ground state. A type of “resonating-VB” cluster-expansion *Ansatz*^{42,43} is an alternative approach to explore. The simplest form of this *Ansatz* limited to nearest-neighbor pairing is essentially that of Pauling and Wheland’s “resonance theory,”²⁵ as applied to π networks of conjugated hydrocarbons, but also applied in physics to the triangular lattice by Anderson and Fazekas.⁴⁴ Further, for the usual structures of these conjugated π networks, it turns out that this simplest resonating-VB *Ansatz* yields⁴⁵ energies more accurate than the corresponding Néel-state energies. Higher-order *Ansätze* in this scheme have been studied³⁹ for infinite linear chains. In terms of the VB approach only qualitative discussions⁴⁶ have been presented concerning the possibility of symmetry-lowering distortion and solitonic excitations.

Here we pursue a more complete VB description. Both the Néel-state-based and resonating-VB cluster-expansion *Ansätze* are applied to the VB model for polyacene. Section II describes the model and the conceivable distortions. Sections III and IV present the *Ansätze* to be used. Section V develops the matrix element formulas for the two types of wave functions. Section VI presents our numerical results (including the effects of elastic distortion) and discussion.

II. POLYACENE MODELS

The polyacene polymer should exhibit some deviation from a perfect chain of regular hexagons (since the symmetry of the overall chain does not require it). If a deviation occurs that lowers the chain’s symmetry, then different symmetry-equivalent distorted ground states may arise. Especially for the extended chain, these different ground states correspond to different (thermodynamic) phases, at sufficiently low temperature, and the

possibility of solitonic excitations and/or conduction could arise. Deviations from planarity often are viewed only to decrease bonding interactions, so we do not consider such distortions here. As a further simplification we presume that translational symmetry is preserved. Both simple CO ideas and simple resonance-theoretic ideas anticipate instabilities under these circumstances. Then the distortions that lower the symmetry would be those that destroy those of the factor group isomorphic to

$$C_{2v} = \{1, C_2, \sigma_v, \sigma_d\}, \quad (2.1)$$

as obtained by factoring the full line group into the translational subgroup and the planar-reflection subgroup. This factor group C_{2v} is that which may be achieved by a single unit cell, as illustrated in Fig. 2.

A catalogue of the possible modes of distortion to be studied is now appropriate. The members of a linearly independent set of such distortion modes may be chosen to transform as irreducible representations of the factor group C_{2v} . Four such distortions we study are associated with the A_1, A_2, B_1, B_2 irreducible representations orthogonal to the “breathing mode” of C_{2v} as indicated in Fig. 3, where only A_1 is totally symmetric. That is, we presently consider only those modes which involve various dilations (or contractions) of individual nearest-neighbor bonds. This is appropriate for the simplest models with only nearest-neighbor interactions. Actually, there are variations in the non-nearest-neighbor interactions (thereby leading to more independent modes), but these changes should be less rapid, roughly in proportion to the relative sizes of the interactions. Thus, within this nearest-neighbor approximation, for the five interactions per unit cell there are five independent distortions. For small distortions, either in the case of the Hückel CO model or of the nearest-neighbor Heisenberg model, the modification of the interactions between pairs of sites can be expressed as

$$g_i \equiv g(r_i) \equiv g_0(1 + \delta_i), \quad (2.2)$$

with

$$\begin{aligned} \delta_1 &\equiv \delta(A_1) + \delta(A_2) + \delta(B_1) + \delta(B_2), \\ \delta_2 &\equiv \delta(A_1) - \delta(A_2) + \delta(B_1) - \delta(B_2), \\ \delta_3 &\equiv \delta(A_1) + \delta(A_2) - \delta(B_1) - \delta(B_2), \\ \delta_4 &\equiv \delta(A_1) - \delta(A_2) - \delta(B_1) + \delta(B_2), \\ \delta_5 &\equiv -4\delta(A_1), \end{aligned} \quad (2.3)$$

where the bonds i are identified as in Fig. 4. Then the

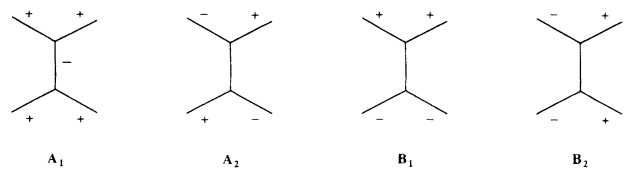


FIG. 2. A unit cell of the polyacene and the reflection symmetries leaving the cell (as a whole) invariant.

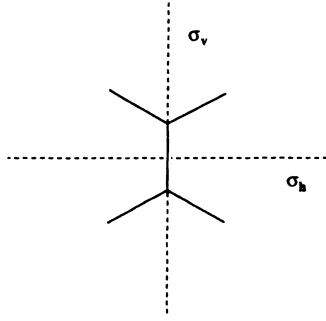


FIG. 3. The four irreducible distortions orthogonal to the “breathing” mode.

models that we consider are of the form

$$H = \sum_n \sum_i (1 + \delta_i) v(r_{ni}) . \quad (2.4)$$

For the Heisenberg (or VB) model

$$v(r_{ni}) = g_0 \mathbf{S}_{nia} \cdot \mathbf{S}_{nib} , \quad (2.5)$$

where \mathbf{S}_{nia} and \mathbf{S}_{nib} are spin operators on sites of subset A and B , respectively, joined by bond i of cell n , and g_0 is the exchange parameter that is taken as a reference. For the Hückel CO model

$$v(r_{ni}) = \beta_0 \sum_{\sigma} (a_{nia\sigma}^{\dagger} a_{nib\sigma} + a_{nib\sigma}^{\dagger} a_{nia\sigma}) , \quad (2.6)$$

where the $a_{nia\sigma}^{\dagger}$ and $a_{nib\sigma}$ are fermion creation and annihilation operators for a spin- σ orbital on sites of subset A and B , respectively, for bond i of unit cell n , and

$$\beta_i \equiv \beta(r_i) \equiv \beta_0 (1 + \delta_i) \quad (2.7)$$

is the resonance-integral (or electron-hopping) parameter.

While the Hückel CO model is readily solved, the VB model is ordinarily only approximately soluble. But in both cases the ground-state energies $\varepsilon((\delta(A_1), \delta(A_2), \delta(B_1), \delta(B_2)))$ per site, in units of g_0 or β_0 , are the aspects of current interest. More particularly the energies

$$\begin{aligned} \varepsilon(A_1, \delta) &\equiv \varepsilon(\delta, 0, 0, 0) , \\ \varepsilon(A_2, \delta) &\equiv \varepsilon(0, \delta, 0, 0) , \\ \varepsilon(B_1, \delta) &\equiv \varepsilon(0, 0, \delta, 0) , \\ \varepsilon(B_2, \delta) &\equiv \varepsilon(0, 0, 0, \delta) , \end{aligned} \quad (2.8)$$

are to be studied as functions of their respective distortions.

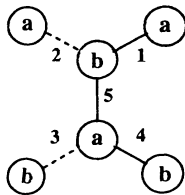


FIG. 4. The labeling convention for the bonds and sites of a unit cell.

tion modes.

To simulate the VB ground-state geometry, we obtain the ground-state equilibrium distances r_i using the two-body nonempirical Heisenberg Hamiltonian for the study of conjugated hydrocarbons,²²

$$\begin{aligned} H &= \sum_n \sum_i [R(r_i) - \frac{1}{2}g(r_i) + 2g(r_i)\mathbf{S}_{nia} \cdot \mathbf{S}_{nib}] \\ &= \sum_n \sum_i [R(r_i) - g(r_i) + g(r_i)\mathcal{P}_{(nia,nib)}] , \end{aligned} \quad (2.9)$$

where $\mathcal{P}_{(nia,nib)}$ is the transposition of spins on sites of subset A and B joined by bond i of unit cell n , and R and g are model parameters incorporating σ and π dependence on the bond length. From the optimal values of r_i , the values of the “irreducible” distortions $\delta(X)$, where $X = A_1, A_2, B_1$, or B_2 , can be obtained readily from (2.2) and (2.3) and values of the $g(r_i)$.

III. NÉEL-STATE-BASED ANSATZ

The cluster-expanded wave-function *Ansatz* in this section is based upon the Néel state

$$|0\rangle = \prod_{n,i} \alpha(nia)\beta(nib) , \quad (3.1)$$

where α and β are spin orbitals, and A and B denote the two sets of sites such that each member of one set is a nearest neighbor solely to sites in the other set. Corrections are made in terms of the (nearest-neighbor) pair-excitation operators

$$P \equiv \sum_{n,i} x_i S_{nia}^- S_{nib}^+ , \quad (3.2)$$

where x_i are scalars to be varied, and S_{nia}^- and S_{nib}^+ are spin raising and lowering operators for sites nia and nib , respectively. The wave-function *Ansatz* is defined

$$|\Phi\rangle \equiv e^{P}|0\rangle . \quad (3.3)$$

This clearly is Néel-state-like with fluctuations away from a pure Néel ordering at an adjacent pair of sites a, b with a probability $\sim x_i^2$.

IV. RESONATING-VB ANSÄTZE

Within one electron per site occupancy, a VB singlet state is defined as a product of pairs of spins coupled to a singlet with no electron unpaired. The set of the linearly independent VB singlet states is⁴⁷ a basis of the subspace of spin-zero states. This is a very large basis set and approximations are needed.

Two asymptotically orthogonal and noninteracting zeroth-order (Kekulé) states, with A_2 and B_2 symmetry, respectively, represented in Fig. 5, can be obtained when pairing is limited to nearest-neighbor spins,

$$\begin{aligned} |K_A\rangle &\equiv \prod_{n,i}^{A_2} (1 - S_{nia}^- S_{nib}^+) |0\rangle , \\ |K_B\rangle &\equiv \prod_{n,i}^{B_2} (1 - S_{nia}^- S_{nib}^+) |0\rangle , \end{aligned} \quad (4.1)$$

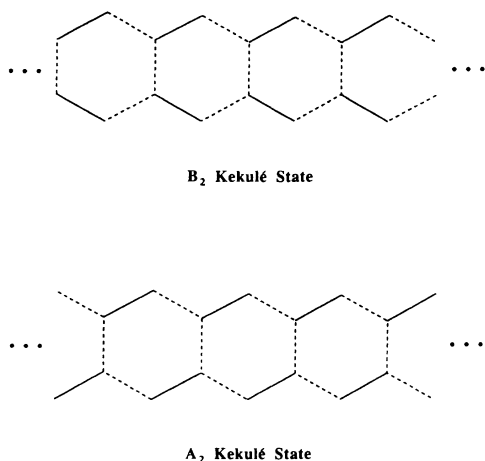


FIG. 5. The two types of symmetry-inequivalent Kekulé states (spin-pair product states).

where the products are over only the solid bonds of Fig. 5.

Since exchange of nearest-neighbor sites results from the Heisenberg Hamiltonian acting on a Kekulé state, a reasonable way to go beyond a Kekulé-state approximation consists of mixing in additional configurations obtained by allowing an arbitrary number of recouplings among adjacent pairings as represented in Fig. 6. Labeling by q_{ef} the operator that leads to the recoupling between adjacent pairs e and f , an overall “higher-order” VB excitation operator can be defined as

$$Q = \sum_{\langle ef \rangle} x_{ef} q_{ef}, \quad (4.2)$$

where x_{ef} is the variational parameter associated to the recoupling of e and f . Then, A - and B -RVB *Ansätze* are defined in terms of Q and the A_2 - and B_2 -symmetry Kekulé states, respectively,

$$|\Phi_X\rangle = U(e^Q)|K_X\rangle, \quad X = A, B, \quad (4.3)$$

where U discards the linked terms of e^Q , namely, those products of q_{ef} where any site index is repeated. The parameters in Q are to be obtained simultaneously upon optimization of the ground-state energy.

V. VB GROUND-STATE ENERGY

Upper bounds to ground-state energy of the system, described by either (2.4) or (2.8) can be obtained upon minimization of

$$E(\Psi) = \frac{\langle \Psi | H | \Psi \rangle}{\langle \Psi | \Psi \rangle} \quad (5.1)$$

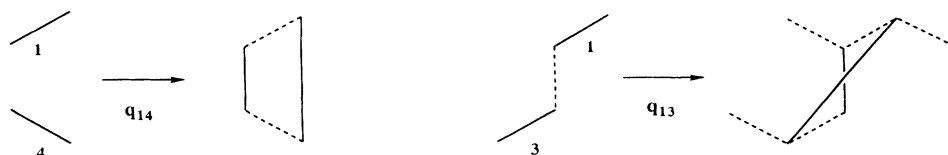


FIG. 6. An example of possible recouplings of pairs of nearest-neighbor singlet spin pairings.

with respect to Ψ , which is selected to be either (3.3) or (4.3).

In order to carry out computations, transfer-matrix techniques⁴⁶ are an extremely useful tool, that allows us to deal with matrix elements in (5.1) locally by unit cells. Effectively, since both the interaction and the *Ansätze* to be used are defined locally, one can introduce local states consisting of possible configurations that can be drawn on a unit cell, containing the contributions from bra and ket parts of $\langle \Psi | \Psi \rangle$. If translational symmetry applies, as is the case, local states are independent of the unit cell, and will be labeled by e_n , where n ranges over the whole set of local states. To account for “propagation” of such local states from the position of one unit cell to the next, it is convenient to define a (position-independent) transfer matrix encoding the local features of the considered *Ansatz* and the system to be studied,

$$T_{nm} \equiv \langle e_n | T | e_m \rangle, \quad (5.2)$$

where T_{nm} is a weighted sum over the various ways a local state e_m in a unit cell may succeed a local state e_n in the previous unit cell. The weight of every term in the sum is the product of variational parameters associated to the particular way e_n evolves to e_m , and, eventually, additional factors proceeding from Pauling’s superpositions rules.⁴⁸

The transfer matrix T is then conveniently used to evaluate the overlap

$$\langle \Psi | \Psi \rangle = \text{tr}(T^L), \quad (5.3)$$

where L is the number of monomer units and we have assumed cyclic boundary conditions. In the long chain limit

$$\langle \Psi | \Psi \rangle \approx \mu^L, \quad (5.4)$$

where μ is the (presumably nondegenerate) largest eigenvalue of T .

Since the operators in the Hamiltonian are local, we can proceed in a similar way as in the overlap to evaluate the matrix elements of the operators in the Hamiltonian. We can define a “connection” matrix on the cells where an interaction takes place and keep the transfer matrix above on the other cells. Connection matrices \underline{C}_i with $i = 1$ to 5, containing the additional features of the single interaction on bond i of some reference unit cell in H , can be defined for every *Ansatz* in such a way that the matrix elements in (5.1) reduce to the sum of the products of \underline{C}_i with a power of T . The connection matrix elements,

$$(\underline{C}_i)_{nm} \equiv \langle e_n | \underline{C}_i | e_m \rangle, \quad (5.5)$$

are obtained as a weighted sum over the various ways a

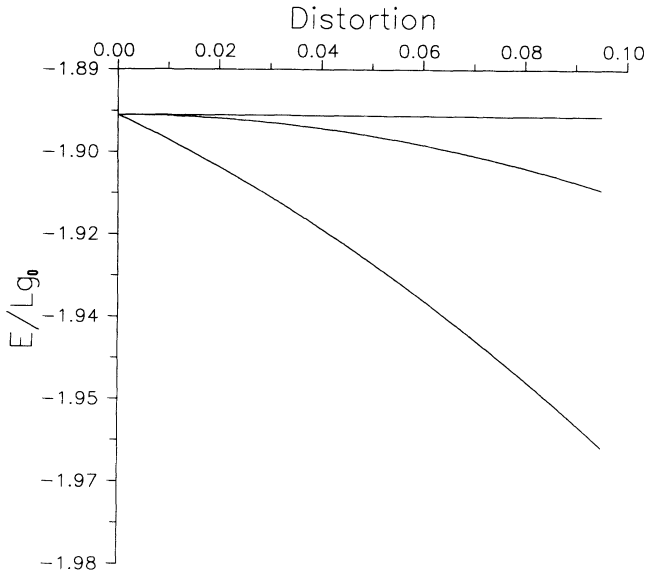


FIG. 7. Néel-state-based *Ansatz* for the irreducible distortions orthogonal to the “breathing” mode. The steep curve is $\epsilon(A_1, \delta)$, the flat one is $\epsilon(B_1, \delta)$, and the parabolic one is $\epsilon(A_2, \delta) = \epsilon(B_2, \delta)$. The curves for nonsymmetric modes are symmetric about $\delta=0$.

local state e_m in the cell just to the right of the interaction on bond i may succeed a local state e_n on the cell just to the left of the interaction. The weight of every term in $(\underline{C}_i)_{nm}$ contains the additional variational parameters originated when proceeding from e_n to e_m through the interaction on bond i . So the Heisenberg Hamiltonian matrix element is expressed as

$$\begin{aligned} \langle \Psi | H | \Psi \rangle &= g_0 L \sum_{i=1}^5 (1 + \delta_i) \langle \Psi | \mathbf{S}_{ia} \cdot \mathbf{S}_{ib} | \Psi \rangle \\ &= g_0 L \sum_{i=1}^5 (1 + \delta_i) \text{tr} \{ \underline{\mathcal{I}}^{L-c_i} \underline{C}_i \}, \end{aligned} \quad (5.6)$$

where c_i is the number of cells involved in \underline{C}_i .

In the long-length limit, the largest eigenvalue μ of $\underline{\mathcal{I}}$ dominates (5.9) and it reduces to

$$\langle \Psi | H | \Psi \rangle \approx g_0 L \sum_{i=1}^5 \mu^{L-c_i} (1 + \delta_i) (\mu, l | \underline{C}_i | \mu, r), \quad (5.7)$$

where $(\mu, l |$ and $|\mu, r)$ are the left and right biorthonormal eigenvectors corresponding to eigenvalue μ of $\underline{\mathcal{I}}$.

Then the Heisenberg energy per unit cell in units of g_0 reduces to

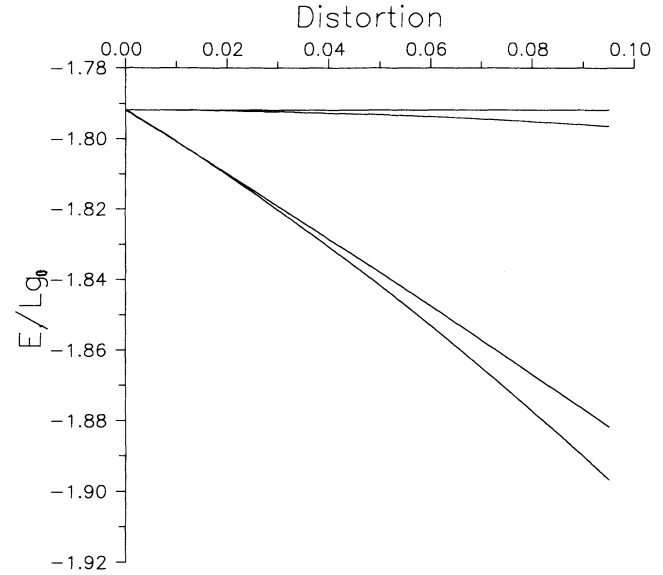


FIG. 8. Resonating valence-bond *Ansätze* for the irreducible distortions orthogonal to the “breathing” mode. The steepest curve is $\epsilon_A(A_1, \delta) = \epsilon_B(A_1, \delta)$, the more moderately sloped steep curve is $\epsilon_A(A_2, \delta) = \epsilon_B(B_2, \delta)$, the parabolic curve is $\epsilon_B(A_2, \delta) = \epsilon_A(B_2, \delta)$, and the flat curve is $\epsilon_A(B_1, \delta) = \epsilon_B(B_1, \delta)$.

$$\epsilon_H \approx \sum_{i=1}^5 \mu^{-c_i} (1 + \delta_i) (\mu, l | \underline{C}_i | \mu, r), \quad (5.8)$$

or, for the nonempirical Hamiltonian (2.8),

$$\epsilon = \sum_{i=1}^5 [R(r_i) - g(r_i) + g(r_i) \mu^{-c_i} (\mu, l | \underline{C}_i | \mu, r)], \quad (5.9)$$

where both r_i and variational parameters in the *Ansatz* are to be obtained upon optimization of the energy.

VI. RESULTS

Using transfer matrices and connection matrices as given in the Appendix, one may compute the energy per unit cell via (5.8) for any of our proposed *Ansätze* at selected values of the δ_i and the variational parameters. With the variation of these *Ansätze* parameters, optimal upper bounds to the ground-state energy are obtained as a function of the δ_i . Via (2.3), δ_i has been computed with the selection of all “irreducible” distortion modes to be zero, but one of them at a time. Hence, the energies designated in (2.7) have been obtained for the three *Ansätze* proposed. The numerical results are shown in Figs. 7 and 8.

It can be seen that ordering of energies for the different

TABLE I. The minimum variationally optimized total energies for each proposed *Ansatz* and associated values of r_i .

<i>Ansatz</i>	$E(\text{cell})$ (eV)	r_1	r_2	r_3 (Å)	r_4	r_5
Néel based	-6.231 74	1.40	1.40	1.40	1.40	1.43
A-RVB	-6.053 87	1.36	1.45	1.36	1.45	1.45
B-RVB	-6.053 87	1.36	1.45	1.45	1.36	1.45

TABLE II. Contributions of the different irreducible distortion modes.

<i>Ansatz</i>	$\delta(A_1)$	$\delta(A_2)$	$\delta(B_1)$	$\delta(B_2)$	$\delta(BR)$
Néel based	0.010 64	0.000 00	0.000 00	0.000 00	-0.023 65
A-RVB	0.020 85	0.106 43	0.000 00	0.000 00	-0.031 85
B-RVB	0.023 57	0.000 00	0.000 00	0.106 43	-0.031 85

“irreducible” distortions orthogonal to the “breathing” mode is the same both for the Néel-state-based *ansatz* and for the RVB ones, though the Néel-state-based *Ansatz* yields Heisenberg energies lower than those obtained by RVB *Ansätze*. Notably, the Néel-state-based *Ansatz* yields a quasilinear δ dependence only for $\varepsilon(A_1, \delta)$, so that no prediction of a distortion is made without consideration of Coulombic and σ -electron contributions to the energy. The Néel-state-based *Ansatz* does, however, share a number of features with the pair of RVB *Ansätze*. First, there is negligible response to the B_1 distortion, and second, the more responsive B_2 and A_2 modes are degenerate. We note that these two qualitative features also occur for the nearest-neighbor tight-binding (or Hückel) model, with arbitrary extents of either distortion, $\delta(A_2)$ or $\delta(B_2)$. Even for the extended Hückel model these conclusions seem to be similar^{7,9,11,12} (though the degeneracy between B_2 and A_2 is not exact).

An argument^{11,12} has, however, been made yielding the alternative conclusion that a Peierls-type B_1 distortion should be favored, this view being based upon a zeroth-order band splitting going to 0 at $k = \pm\pi$ from the Hückel model, and a nonzero distortive-response matrix element from some sort of extended Hückel model. Both the splitting and distortive matrix element are *accidentally* zero for the Hückel model, while for the extended Hückel model both are nonzero (though small), so that for either of these (unmixed) models a Peierls distortion is avoided. We believe the argument to use the “mixed” model is weak, and the resultant predictions are in disagreement with pure CO models and both of our present approximate results for the VB model.

To make a more comprehensive VB treatment the effects of Coulombic and σ -electron interactions need to be taken into account. This we do using the model of Said *et al.*²² as in (2.9), and thereby we obtain the ground-state geometry upon searching out (as a function of the r_i) the minimum variationally optimized total energy for each proposed *Ansatz*. These minimum total energies and associated values of r_i are presented in Table I, while in Table II the contributions of the different irreducible distortion modes, including the “breathing” with

respect to benzene, are given for these minimum energies. For the Néel-state-based *Ansatz* we find any nonsymmetric distortion to be entirely negligible. But the pair of RVB *Ansätze* yield degenerate A_2 and B_2 distortions, though at higher energies, and so may be viewed as not so favorable. It is perhaps not too surprising that the Néel-state-based *Ansatz* is superior. Upon examination of earlier argued⁴⁵ (sufficient) criteria for preference of the RVB description, one finds that for polyacene both the coordinate-number criterion ($z \leq 3$) and the benzenoid ring criterion are met, but the criterion of a high density of Kekulé structures is not. However, the criteria for preference of a Néel-state-based solution also are not (fully) met, and since the present Néel-state-based *Ansatz* yields energies only slightly lower than our RVB *Ansätze*, the question of the nature of the exact ground state is not fully clear, especially upon inclusion of higher-order (non-nearest-neighbor RVB-favoring) corrections to the Heisenberg (or VB) model. In the absence both of such higher-order corrections and of bond-length distortions, one may gain some better indication of relative accuracies through comparison to results for corresponding *Ansätze*^{30,39} applied to the linear-chain Heisenberg model, whose exact solution is known.³² This comparison for energies per site (in units of g_0) is made in Table III. The last number there (in parentheses) is our guess based both on comparison and on the better satisfaction of the higher coordination number criterion⁴⁵ for enhancement of Néel-state-based results. Our cluster-expansion *Ansätze* notably improve upon single Néel and Kekulé states.

Overall our present work indicates either a symmetric ground-state geometry or one with slight A_2 and/or B_2 distortions which are exactly degenerate within our approximation. The asymmetric distortion mode recommended by Kivelson and Chapman¹¹ and by Božović¹² is not favored. The degeneracy of low-energy A_2 and B_2 distortion modes indicates the possibility of novel solitonic excitations, if not for bare polyacene then at least for the polymer when subjected to suitable chemical perturbations. The qualitative characteristics for the VB picture seem not too dissimilar to that in a band-theoretic

TABLE III. A comparison of the results for corresponding *Ansätze* applied to the linear-chain Heisenberg model for energies per site (in units of g_0).

	Linear chain	Polyacene
Néel state	-0.2500	-0.3125
Kekulé state	-0.3750	-0.3750
RVB cluster <i>Ansatz</i>	-0.4269	-0.4480
Néel cluster <i>Ansatz</i>	-0.4374	-0.4740
exact	-0.4431	(-0.48)

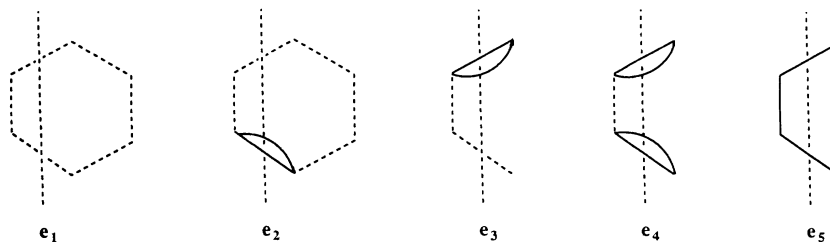


FIG. 9. The local states for the Néel-state-based *Ansatz*. The longer vertical dashed line simply marks a chosen position within each unit cell. The solid lines crossing this dashed line indicate pair excitations (in bra or ket).

picture, either at the Hückel model of approximation or even at the extended-Hückel level.

ACKNOWLEDGMENTS

M.A.G.B. acknowledges support from DGICYT (Project No. PS90-0061) and CIRIT (Generalitat de Catalunya, EE-90/1), and also Professor J.-P. Malrieu's valuable comments; D.J.K. acknowledges support from the Welch Foundation of Houston, Texas.

APPENDIX

Five local states in Fig. 9 can be readily identified for the Néel-based *Ansatz*. Hence, if e_n and e_m are the first and second local states of Fig. 9, then there are two manners that e_m may follow e_n as indicated in Fig. 10; the associated weights involved in proceeding from e_n to e_m are there seen to be x_4^2 and $x_2^2 x_4^2$, so that

$$T_{1,2} = x_4^2 + x_2^2 x_4^2. \quad (\text{A1})$$

Proceeding similarly for the other matrix elements we find the whole transfer matrix

$$\underline{T} = \begin{pmatrix} y_2 y_3 + x_5^2 & y_2 x_4^2 & x_1^2 y_3 & x_1^2 x_4^2 & 2x_1 x_4 x_5 \\ y_2 + x_5^2 & y_2 x_4^2 & x_1^2 & x_1^2 x_4^2 & 2x_1 x_4 x_5 \\ y_3 + x_5^2 & x_4^2 & x_1^2 y_3 & x_1^2 x_4^2 & 2x_1 x_4 x_5 \\ y_5 & x_4^2 & x_1^2 & x_1^2 x_4^2 & 2x_1 x_4 x_5 \\ x_2 x_3 x_5 & 0 & 0 & 0 & x_1 x_2 x_3 x_4 \end{pmatrix}, \quad (\text{A2})$$

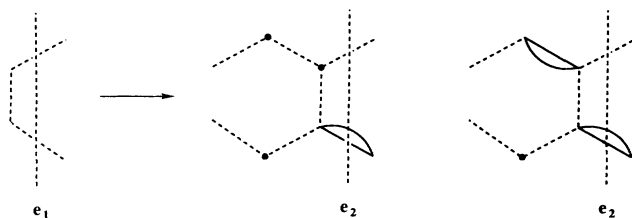


FIG. 10. The two possible ways in which an e_2 local state may follow an e_1 local state.

where we have abbreviated

$$y_i \equiv 1 + x_i^2. \quad (\text{A3})$$

Next, when the operator for bond i is selected to be the transposition operator, connection matrices can be written as

$$\underline{C}_1 = \frac{\partial \underline{T}}{\partial x_1} + \frac{1}{\mu} \{ [\underline{T}(1) - \underline{T}(1,2,5)] \underline{T}(2) + \underline{T}(1,2,5) [\underline{T} - \underline{T}(2)] \}, \quad (\text{A4})$$

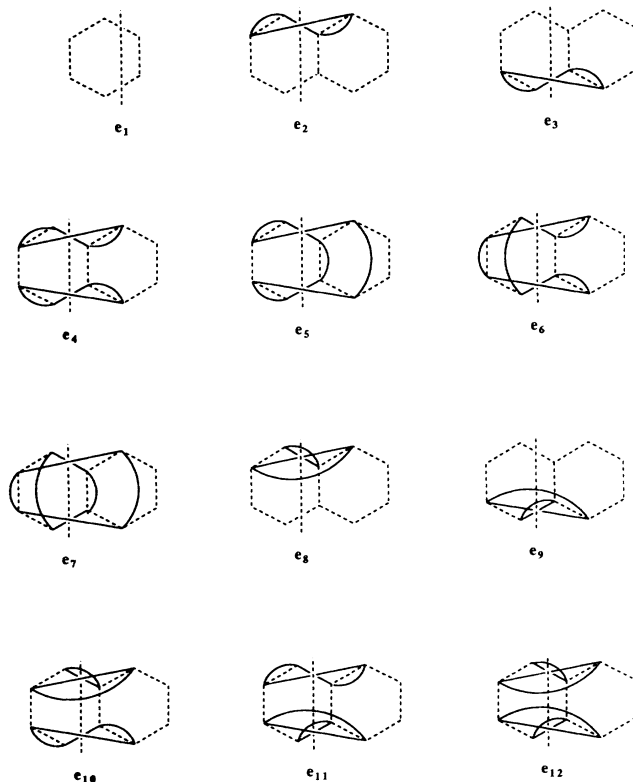


FIG. 11. The local states for the *B-RVB Ansatz*. Again, the longer dashed line marks positions. The solid lines crossing this dashed line indicate (singlet) spin pairings (in bra or ket).

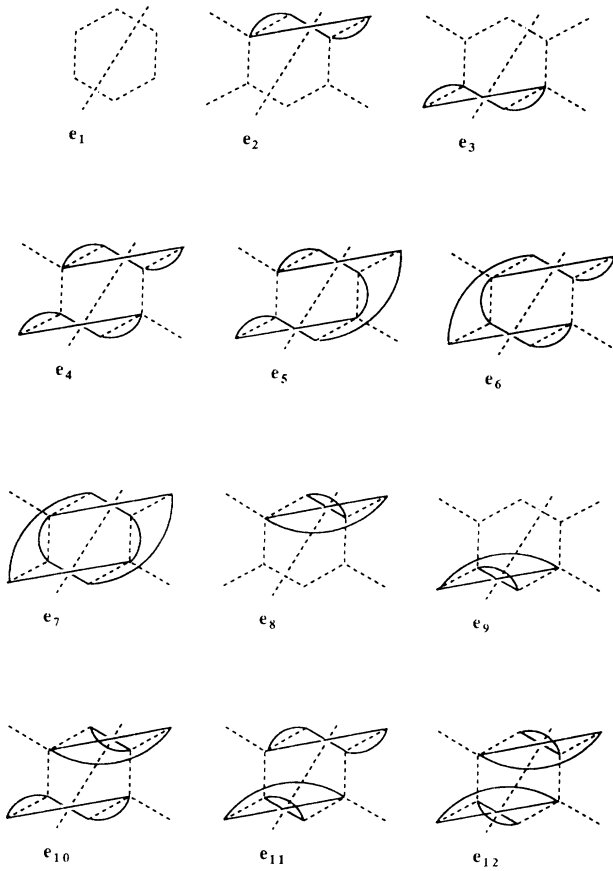


FIG. 12. The local states for the *A*-RVB Ansatz.

$$\underline{C}_2 = \frac{\partial T}{\partial x_2} + \frac{1}{\mu} \{ [T - T(1)]T(1,2,5) + T(1)[T(2) - T(1,2,5)] \}, \quad (A5)$$

$$\underline{C}_3 = \frac{\partial T}{\partial x_3} + \frac{1}{\mu} \{ [T - T(4)]T(3,4,5) + T(4)[T(3) - T(3,4,5)] \}, \quad (A6)$$

$$\underline{C}_4 = \frac{\partial T}{\partial x_4} + \frac{1}{\mu} \{ [T(4) - T(3,4,5)]T(3) + T(3,4,5)[T - T(3)] \}, \quad (A7)$$

$$\underline{C}_5 = \frac{\partial T}{\partial x_5} + [T(3,4,5) + T(1,2,5) - 2T(1,2,3,4,5)], \quad (A8)$$

where the notation $T(i)$ indicates the matrix T with x_i set to 0 and $T(i, j, k)$ indicates T with $x_i = x_j = x_k = 0$.

For either A_2 or B_2 RVB Ansatz we obtain twelve local states. With an adequate one-to-one correspondence between the two basis sets (as in Figs. 11 and 12) and between the variational parameters involved (as in Figs. 13 and 14) it is possible to have the same T matrix for both RVB Ansatz:

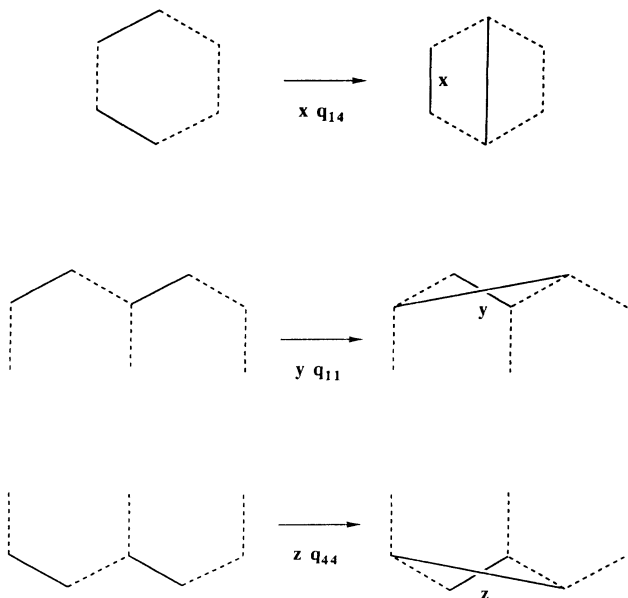


FIG. 13. The parametrization for the pair recouplings of pairs of nearest-neighbor spin pairings for the *B*-RVB Ansatz.

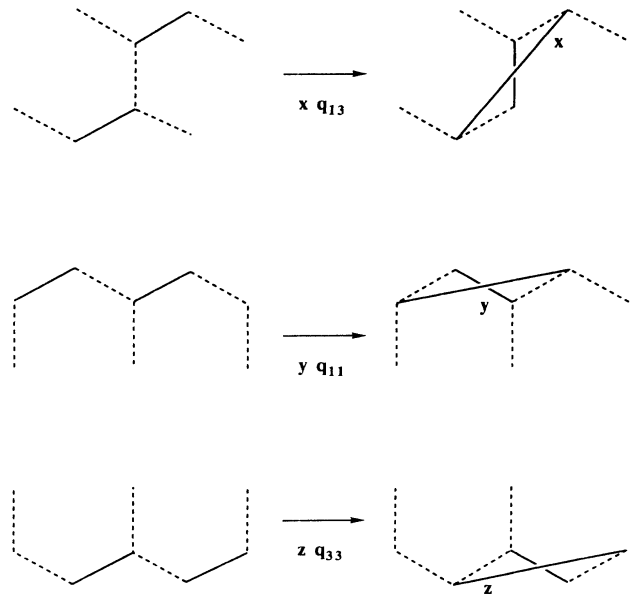


FIG. 14. The parametrization associated to the *A*-RVB Ansatz.

$$\underline{T} = \begin{pmatrix} 4(1+x+x^2) & 2y(2+x) & 2z(2+x) & 4yz & 2yz & 2xyz & 2xyz & 2y^2 & 2z^2 & 2y^2z & 2yz^2 & y^2z^2 \\ 2(2+x) & 2y & z(4+x) & 2yz & yz & 0 & 0 & 0 & 2z^2 & 0 & yz^2 & 0 \\ 2(2+x) & y(4+x) & 2z & 2yz & yz & 0 & 0 & 2y^2 & 0 & y^2z & 0 & 0 \\ 4 & 2y & 2z & yz & 0 & 0 & 0 & 0 & 0 & 0 & 0 & 0 \\ 2x & 0 & 0 & 0 & yz & 0 & 0 & 0 & 0 & 0 & 0 & 0 \\ 2 & y & z & 0 & 0 & yz & 0 & 0 & 0 & 0 & 0 & 0 \\ 4x & 0 & 0 & 0 & 0 & 0 & yz & 0 & 0 & 0 & 0 & 0 \\ 8 & 0 & 8z & 0 & 0 & 0 & 0 & 0 & 4z^2 & 0 & 0 & 0 \\ 8 & 8y & 0 & 0 & 0 & 0 & 0 & 4y^2 & 0 & 0 & 0 & 0 \\ 8 & 0 & 4z & 0 & 0 & 0 & 0 & 0 & 0 & 0 & 0 & 0 \\ 8 & 4y & 0 & 0 & 0 & 0 & 0 & 0 & 0 & 0 & 0 & 0 \\ 16 & 0 & 0 & 0 & 0 & 0 & 0 & 0 & 0 & 0 & 0 & 0 \end{pmatrix} .$$

(A9)

Also, it can be seen that, with the correspondence suggested above,

$$\underline{C}_i(A_2) = \underline{C}_i(B_2), \quad i = 1, 2, 5,$$

$$\underline{C}_3(A_2) = \underline{C}_4(B_2),$$

$$\underline{C}_4(A_2) = \underline{C}_3(B_2),$$

(A10)

with

$$c_i(B_2) = \begin{cases} 2, & i = 2, 3 \\ 1, & i = 1, 4, 5. \end{cases} \quad (\text{A11})$$

Specifically the matrices are

$$\underline{C}_1(7, 8, 10, 12) = \begin{pmatrix} 4(1+x) & 2y(2+x) & 2z(2+x) & 4yz & 2yz & 2xyz & 2z^2 & 2yz^2 \\ 2(2+x) & 2y & z(4+x) & 2yz & yz & 0 & 2z^2 & yz^2 \\ 2(2+x) & y(4+x) & 2z & 2yz & yz & 0 & 0 & 0 \\ 4 & 2y & 2z & yz & 0 & 0 & 0 & 0 \\ 2x & 0 & 0 & 0 & yz & 0 & 0 & 0 \\ 2 & y & z & 0 & 0 & yz & 0 & 0 \\ 8 & 8y & 0 & 0 & 0 & 0 & 0 & 0 \\ 8 & 4y & 0 & 0 & 0 & 0 & 0 & 0 \end{pmatrix} ,$$

(A12)

$$\underline{C}_4(7, 9, 11, 12) = \begin{pmatrix} 4(1+x) & 2y(2+x) & 2z(2+x) & 4yz & 2yz & 2xyz & 2y^2 & 2y^2z \\ 2(2+x) & 2y & z(4+x) & 2yz & yz & 0 & 0 & 0 \\ 2(2+x) & y(4+x) & 2z & 2yz & yz & 0 & 2y^2 & y^2z \\ 4 & 2y & 2z & yz & 0 & 0 & 0 & 0 \\ 2x & 0 & 0 & 0 & yz & 0 & 0 & 0 \\ 2 & y & z & 0 & 0 & yz & 0 & 0 \\ 8 & 0 & 8z & 0 & 0 & 0 & 0 & 0 \\ 8 & 0 & 4z & 0 & 0 & 0 & 0 & 0 \end{pmatrix} ,$$

(A13)

$$\underline{C}_5(4, 8, 9, 10, 11, 12) = \begin{pmatrix} 4(1+x) & 2xy & 2xz & 2yz & 2xyz & 2xyz \\ 2x & 0 & xz & yz & 0 & 0 \\ 2x & xy & 0 & yz & 0 & 0 \\ 2x & 0 & 0 & 0 & yz & 0 \\ 2 & y & z & 0 & 0 & yz \\ 4x & 0 & 0 & 0 & 0 & 0 \end{pmatrix}, \quad (\text{A14})$$

$$\underline{C}_2(8, 10, 12, 3, 10) = \begin{pmatrix} 4x^2 & 2y[\mu(2+x)+zx^2] & 4\mu yz & 2yz(\mu+xz) & 2\mu xyz & 2\mu xyz & 2\mu y^2 & 2\mu y^2 z & 2\mu yz^2 & \mu y^2 z^2 \\ 2x^2 & y(2\mu+zx^2) & 2\mu yz & yz(\mu+xz) & 0 & 0 & 0 & 0 & \mu yz^2 & 0 \\ 0 & \mu y(4+x) & 2\mu yz & \mu yz & 0 & 0 & 2\mu y^2 & \mu y^2 z & 0 & 0 \\ 0 & 2\mu y & \mu yz & 0 & 0 & 0 & 0 & 0 & 0 & 0 \\ 0 & 0 & 0 & \mu yz & 0 & 0 & 0 & 0 & 0 & 0 \\ 2x & y(\mu+xz) & 0 & yz^2 & \mu yz & 0 & 0 & 0 & 0 & 0 \\ 0 & 0 & 0 & 0 & 0 & \mu yz & 0 & 0 & 0 & 0 \\ 0 & 8\mu y & 0 & 0 & 0 & 0 & 4\mu y^2 & 0 & 0 & 0 \\ 0 & 4\mu y & 0 & 0 & 0 & 0 & 0 & 0 & 0 & 0 \end{pmatrix}, \quad (\text{A15})$$

$$\underline{C}_3(9, 11, 12; 2, 8) = \begin{pmatrix} 4x^2 y & 2z[\mu(2+x)+x^2 y] & 4\mu yz & 2yz(\mu+xy) & 2\mu xyz & 2\mu xyz & 2\mu z^2 & 2\mu y^2 z & 2\mu yz^2 & \mu y^2 z^2 \\ 0 & \mu z(4+x) & 2\mu yz & \mu yz & 0 & 0 & 2\mu z^2 & 0 & \mu yz^2 & 0 \\ 2x^2 y & z(2\mu+x^2 y) & \mu yz & yz(\mu+xy^2) & 0 & 0 & 0 & \mu y^2 z & 0 & 0 \\ 0 & 2\mu z & \mu yz & 0 & 0 & 0 & 0 & 0 & 0 & 0 \\ 0 & 0 & 0 & \mu yz & 0 & 0 & 0 & 0 & 0 & 0 \\ 2xy & z(\mu+xy) & 0 & 0 & \mu yz & 0 & 0 & 0 & 0 & 0 \\ 0 & 0 & 0 & y^2 z & 0 & \mu yz & 0 & 0 & 0 & 0 \\ 0 & 8\mu z & 0 & 0 & 0 & 0 & 4\mu z^2 & 0 & 0 & 0 \\ 0 & 4\mu z & 0 & 0 & 0 & 0 & 0 & 0 & 0 & 0 \end{pmatrix}, \quad (\text{A16})$$

where a parenthetical label identifies rows and columns of zeros which have been suppressed in our presentation. For example, $(i, j; k)$ indicates that rows i and j as well as column k are all zero and have been deleted. Hence, it can be easily shown that

$$\varepsilon_A(X_1, \delta) = \varepsilon_B(X_1, \delta), \quad X = A, B \quad (\text{A17})$$

$$\varepsilon_A(A_2, \delta) = \varepsilon_B(B_2, \delta), \quad (\text{A18})$$

and

$$\varepsilon_B(A_2, \delta) = \varepsilon_A(B_2, \delta). \quad (\text{A19})$$

¹C. A. Coulson, Proc. Phys. Soc. London Sect. A **60**, 257 (1948).

²R. McWeeny, Proc. Phys. Soc. London Sect. A **65**, 839 (1952).

³W. Moffitt, J. Chem. Phys. **22**, 1820 (1954).

⁴L. Salem and H. C. Longuet-Higgins, Proc. R. Soc. London Ser. A **255**, 435 (1960).

⁵M. Kimura, H. Kawabe, K. Nishikawa, and S. Aano, J. Chem. Phys. **85**, 3090 (1986).

⁶M. R. Boon, Theor. Chim. Acta **23**, 109 (1971).

⁷M-H. Whangbo, R. Hoffmann, and R. B. Woodward, Proc. R. Soc. London Ser. A **366**, 23 (1979).

⁸M. Kertesz and R. Hoffmann, Solid State Commun. **47**, 97 (1983); M. Kertesz, Y. S. Lee, and J. J. P. Stewart, Int. J. Quantum Chem. **35**, 305 (1989).

⁹K. Tanaka, K. Ohzeki, S. Nankai, T. Yamabe, and H. Shirakawa, J. Phys. Chem. Solids **44**, 1069 (1983).

¹⁰A. L. S. da Rosa and C. P. de Melo, Phys. Rev. B **38**, 5430 (1988).

¹¹S. Kivelson and O. L. Chapman, Phys. Rev. B **28**, 7236 (1983).

¹²I. Božović, Phys. Rev. B **32**, 8136 (1985).

¹³P. Tavan and K. Schulten, J. Chem. Phys. **70**, 5414 (1979).

¹⁴M. Baldo, A. Grassi, R. Pucci, and P. Tomasello, J. Chem. Phys. **77**, 2438 (1982).

¹⁵M. Baldo, G. Piccitto, R. Pucci, and P. Tomasello, Phys. Lett. **95A**, 201 (1983).

¹⁶R. Pucci and N. H. March, Phys. Lett. **94A**, 63 (1983).

¹⁷P. W. Anderson, Phys. Rev. **115**, 1 (1959).

- ¹⁸R. D. Poshsuta and D. J. Klein, *Phys. Rev. Lett.* **48**, 1555 (1982).
- ¹⁹S. Kuwajima, *J. Chem. Phys.* **77**, 1030 (1982).
- ²⁰J. P. Malrieu and D. Maynau, *J. Am. Chem. Soc.* **104**, 3021 (1982).
- ²¹D. Maynau and J. P. Malrieu, *J. Am. Chem. Soc.* **104**, 3029 (1982).
- ²²M. Said, D. Maynau, J.-P. Malrieu, and M. A. Garcia-Bach, *J. Am. Chem. Soc.* **106**, 571 (1984).
- ²³L. Pauling and G. W. Wheland, *J. Chem. Phys.* **1**, 362 (1933).
- ²⁴H. Eyring, J. Walter, and G. E. Kimball, *Quantum Chemistry* (Wiley, New York, 1942).
- ²⁵G. W. Wheland, *Resonance in Organic Chemistry* (Wiley, New York, 1955).
- ²⁶*Valence-Bond Theory and Chemical Structure*, edited by D. J. Klein and N. Trinajstić (Elsevier, Amsterdam, 1990).
- ²⁷W. A. Seitz, D. J. Klein, T. G. Schmalz, and M. A. Garcia-Bach, *Chem. Phys. Lett.* **115**, 139 (1986).
- ²⁸W. A. Seitz and T. C. Schmalz, in *Valence-Bond Theory and Chemical Structure* (Ref. 26), pp. 525–551.
- ²⁹D. J. Klein, T. G. Schmalz, W. A. Seitz, and G. E. Hite, *Int. J. Quantum Chem.* **19**, 707 (1986).
- ³⁰D. J. Klein and M. A. Garcia-Bach, *Phys. Rev. B* **19**, 877 (1989).
- ³¹S. Ramasesha and Z. G. Soos, *Int. J. Quantum Chem.* **25**, 1003 (1984); S. A. Alexander and T. G. Schmalz, *J. Am. Chem. Soc.* **109**, 6933 (1987).
- ³²L. Hulthén, *Ark. Mat. Astron. Fys. A* **26**, 1 (1938).
- ³³P. W. Kasteleyn, *Physica (Utrecht)* **18**, 104 (1952).
- ³⁴D. A. Huse and V. Elser, *Phys. Rev. Lett.* **60**, 2531 (1988).
- ³⁵C. Vroelant and R. Daudel, *Bull. Soc. Chim. Fr.* **16**, 36 (1949).
- ³⁶I. Nebenzahl, *Phys. Rev.* **177**, 1001 (1969).
- ³⁷R. R. Bartkowski, *Phys. Rev. B* **5**, 4536 (1972).
- ³⁸D. J. Klein, *Mol. Phys.* **31**, 811 (1976).
- ³⁹D. J. Klein and M. A. Garcia-Bach, *Int. J. Quantum Chem.* **64**, 4873 (1976).
- ⁴⁰P. W. Anderson, *Science* **235**, 1196 (1987).
- ⁴¹E. H. Lieb and D. C. Mattis, *J. Math. Phys. (N.Y.)* **3**, 749 (1962).
- ⁴²D. J. Klein, *Phys. Rev. B* **19**, 870 (1979).
- ⁴³S. Liang, B. Douçot, and P. W. Anderson, *Phys. Rev. Lett.* **61**, 365 (1988).
- ⁴⁴P. W. Anderson, *Mater. Res. Bull.* **8**, 153 (1975); P. Fazekas and P. W. Anderson, *Philos. Mag.* **30**, 423 (1974).
- ⁴⁵D. J. Klein, S. A. Alexander, W. A. Seitz, T. G. Schmalz, and G. E. Hite, *Theor. Chim. Acta* **69**, 393 (1986).
- ⁴⁶D. J. Klein, G. E. Hite, and T. G. Schmalz, *J. Comput. Chem.* **7**, 443 (1986); D. J. Klein, M. A. Garcia-Bach, and W. A. Seitz, *J. Mol. Struct.* **185**, 287 (1989).
- ⁴⁷G. Rümer, *Nachr. Ges. Wiss. Göttingen Math. Physik. Kl.* **337** (1932).
- ⁴⁸L. Pauling, *J. Chem. Phys.* **1**, 280 (1933).